Published June 27, 2011

FoxM1 mediates the progenitor function of type II epithelial cells in repairing alveolar injury induced by *Pseudomonas aeruginosa*

Yuru Liu,[1] Ruxana T. Sadikot,[2,4] Guy R. Adami,[3] Vladimir V. Kalinichenko,[5,6] Srikanth Pendyala,[1] Viswanathan Natarajan,[1] You-yang Zhao,[1] and Asrar B. Malik[1]

[1]Department of Pharmacology and [2]Department of Medicine, College of Medicine; and [3]Department of Oral Medicine and Diagnostic Science, College of Dentistry; University of Illinois at Chicago, Chicago, IL 60612
[4]Jesse Brown Veterans Affairs Medical Center, Chicago, IL 60612
[5]Division of Pulmonary Biology and [6]Perinatal Institute, Cincinnati Children's Hospital Research Foundation, Cincinnati, OH 45229

The alveolar epithelium is composed of the flat type I cells comprising 95% of the gas-exchange surface area and cuboidal type II cells comprising the rest. Type II cells are described as facultative progenitor cells based on their ability to proliferate and trans-differentiate into type I cells. In this study, we observed that pneumonia induced by intratracheal instillation of *Pseudomonas aeruginosa* (PA) in mice increased the expression of the forkhead transcription factor *FoxM1* in type II cells coincidentally with the induction of alveolar epithelial barrier repair. FoxM1 was preferentially expressed in the Sca-1$^+$ subpopulation of progenitor type II cells. In mice lacking *FoxM1* specifically in type II cells, type II cells showed decreased proliferation and impaired trans-differentiation into type I cells. Lungs of these mice also displayed defective alveolar barrier repair after injury. Expression of FoxM1 in the knockout mouse lungs partially rescued the defective trans-differentiation phenotype. Thus, expression of FoxM1 in type II cells is essential for their proliferation and transition into type I cells and for restoring alveolar barrier homeostasis after PA-induced lung injury.

CORRESPONDENCE
Asrar B. Malik:
abmalik@uic.edu
OR
Yuru Liu:
yuruliu@uic.edu

Abbreviations used: BAL, bronchoalveolar lavage; i.t., intratracheal(ly); mRNA, messenger RNA; PA, *Pseudomonas aeruginosa*; SAP, surfactant-associated protein.

The mechanism of epithelial regeneration varies among organs. In the skin and intestine, niches for resident stem cells ensure rapid renewal of epithelial cell populations upon tissue injury (Blanpain et al., 2004; Barker and Clevers, 2007). In the liver, pancreas, and lungs, epithelial cells have a relatively slow renewal capacity (Dor et al., 2004; Erker and Grompe, 2008; Stripp, 2008). Populations of functionally differentiated cells termed facultative progenitor cells can be activated upon injury to enter the cell cycle and give rise to epithelial cells (Dor et al., 2004; Erker and Grompe, 2008). In the airway epithelium, specific cells act as progenitor cells to repair different regions of airways. Clara cells of upper airways normally function to secrete mucus but also play a role in the repair (Rawlins and Hogan, 2006; Stripp, 2008; Rawlins et al., 2009a). The lung alveolar epithelium is composed of type I cells that make up 95% of the alveolar surface area and type II cells making up the remainder (Mason, 2006). Upon alveolar epithelial injury, differentiated type II cells are activated to induce epithelial barrier repair (Rawlins and Hogan, 2006; Stripp, 2008). These cells upon entering the cell cycle give rise to both type II and type I cells (Mason, 2006; Rawlins and Hogan, 2006; Sugahara et al., 2006; Stripp, 2008). Studies using NO_3 to injure alveoli showed that ^3H first labeled proliferating type II cells and later type I cells (Evans et al., 1973, 1975). Cultured type II cells were also shown to trans-differentiate directly into type I cells (Dobbs, 1990; Paine and Simon, 1996).

Alveolar epithelial injury responsible for the acute respiratory distress syndrome occurs secondary to the release of proinflammatory

The Rockefeller University Press $30.00
J. Exp. Med. Vol. 208 No. 7 1473-1484
www.jem.org/cgi/doi/10.1084/jem.20102041

Supplemental Material can be found at:
http://jem.rupress.org/content/suppl/2011/06/23/jem.20102041.DC1.html

Published June 27, 2011

cytokines as well as proteases and oxidants (Ware and Matthay, 2000). However, little is known about the transcriptional machinery directing the alveolar repair program. FoxM1 (or foxm1b), a member of the mammalian forkhead box family of transcription factors, upon activation induces G1/S transition by decreasing the expression of nuclear cyclin-dependent kinase inhibitor proteins p27kip and p21Cip (Costa et al., 2005). FoxM1 also induces expression of genes essential for G2/M phase of the cell cycle, CDC25b, cyclin B1, Polo-like kinase 1, and Aurora B kinase (Costa et al., 2005). Based on the role of FoxM1 in mediating morphogenesis and differentiation of the embryonic lung (Kim et al., 2005a; Kalin et al., 2008) and in repairing the lung endothelial barrier after LPS-induced injury (Zhao et al., 2006), in this study, we addressed the function of FoxM1 in the mechanism of alveolar epithelial barrier repair.

Using the *Pseudomonas aeruginosa* (PA) model of lung alveolar injury (Gray and Kreger, 1979; Sadikot et al., 2006), we found that *FoxM1* expression in type II cells after PA challenge was coupled to increased type II cell proliferation and reannealing of the alveolar epithelial barrier. FoxM1 was also preferentially expressed in the Sca-1$^+$ (for stem cell antigen 1; Holmes and Stanford, 2007) progenitor subfraction of type II cells. Inactivation of *FoxM1* in type II alveolar cells in mice prevented type II cell proliferation and their trans-differentiation into type I cells, resulting in prolonged alveolar barrier dysfunction. In a rescue experiment, expression of FoxM1 in the knockout mice partially restored the trans-differentiation defect. Thus, FoxM1 is required for the progenitor cell function of type II epithelial cells and repairing of the alveolar epithelial barrier after PA-induced lung injury.

RESULTS

FoxM1 expression in type II cells during alveolar epithelial repair after PA exposure

To study mechanisms of alveolar epithelial repair, we used an established mouse airspace injury model generated by intratracheal (i.t.) injection of PA (strain 103; Sadikot et al., 2006). Death of alveolar epithelial cells was observed at 24 h after infection (Fig. S1, A–C). Acute lung inflammation and increased cell density were observed at 48–96 h after PA challenge, and the most severe changes were seen at 72 h (Fig. 1, A–F). At 7 d after infection, normal airspace morphology was restored (Fig. 1 F). A previous study showed that the maximum inflammatory response occurred at 24–48 h in PA-treated mice (Sadikot et al., 2006); thus, the increased number of cells at 72 and 96 h may reflect cell proliferation occurring during the repair phase. Using BrdU labeling to identify proliferating cells, we observed that the number of BrdU$^+$ cells was significantly increased at 72 h after infection (Fig. S1, D and E), indicating that the lungs are actively engaged in repair at this time. By double labeling with antibodies against BrdU and type II cell marker Sp-C (for surfactant-associated protein [SAP] C; Wert et al., 1993), we found that the type II cell proliferation rate was significantly increased at 72 h, which is the beginning of the repair phase (Fig. 1, G–I). These results support the concept that a type II cell can function as a progenitor cell during alveolar repair (Mason, 2006; Sugahara et al., 2006).

Type II cells were isolated after PA infection, and RNA was prepared for real-time RT-PCR analysis. *FoxM1* transcript amounts started to increase at 48 h, peaked at 72 h, and decreased at 96 h (Fig. 2 A). In contrast, type II cell expression of several other genes, *Sp-C* (Wert et al., 1993), *CC10* (Rawlins et al., 2009a), *Gata6* (Zhang et al., 2008), *Id2* (Liu and Hogan, 2002; Rawlins et al., 2009b), *Elf5* (Metzger et al., 2008), *Erm* (Liu et al., 2003), and *E-cadherin* (Reddy et al., 2004), did

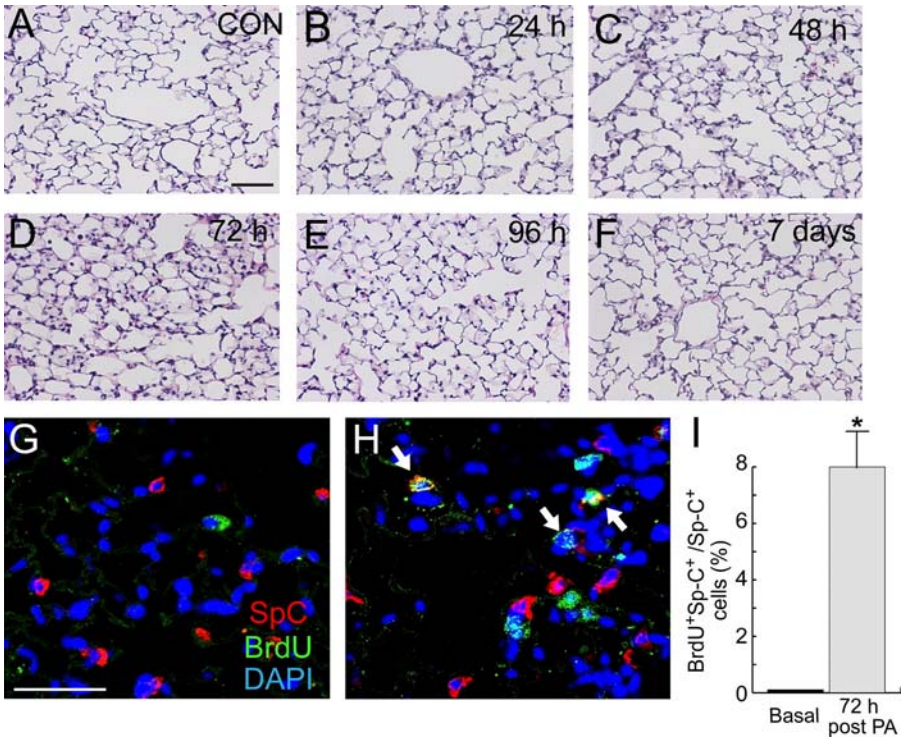

Figure 1. Morphology and cell proliferation after PA-induced lung injury. (A–F) Lung sections were prepared for control (CON; A) and at 24 h (B), 48 h (C), 72 h (D), 96 h (E), and 7 d (F) after i.t. injection of PA and processed for H&E staining. (G and H) BrdU and Sp-C double labeling of control lungs (G) and lungs at 72 h after PA injection (H). DAPI was used to show nuclei. Arrows denote proliferative type II cells (double positive for Sp-C and BrdU). Results are representative of similar observations from three independent experiments. Bars: (A–F) 60 µm; (G and H) 20 µm. (I) Percentage of BrdU$^+$Sp-C$^+$ cells among the Sp-C$^+$ cells in noninfected (Basal) and 72-h-postinfected lungs. Data are presented as mean ± SE (*, $P < 0.05$ vs. control). More than 500 cells were scored in each sample ($n = 5$ mice for each group from three independent experiments).

Published June 27, 2011

not show clear changes at 72 h after infection (Fig. S2). Importantly, expression of *FoxM1* in type I cells did not increase at 72 h after infection (Fig. 2 B). Thus, the expression of *FoxM1* increased specially and significantly only in type II cells during the repair phase.

FoxM1 is preferentially expressed in the Sca-1$^+$ subgroup of type II cells

Because the type II cell subpopulation may function as facultative progenitor cells during alveolar repair, we determined whether the FoxM1-expressing type II cells concomitantly expressed Sca-1, a marker of progenitor cells (Holmes and Stanford, 2007). Sca-1 was analyzed by FACS in freshly isolated type II cells before and at 72 h after infection using PE-labeled rat anti–Sca-1 mAb (Raiser and Kim, 2009). Few Sca-1$^+$ type II cells were present in control lungs, whereas Sca-1$^+$ cell number increased significantly at 72 h after PA (Fig. 3, A and B); the percentage of Sca-1$^+$ cells in type II cells was as high as 60%. Notably, most Sca-1$^+$ cells also expressed the type II cell marker Sp-C (Fig. 3 C). Furthermore, most of the Sca-1$^+$ cells showed positive staining for epithelial cell markers E-cadherin and pan-cytokeratin (Fig. 3, D and E; Willis et al., 2005), indicating that these were epithelial cells. To determine whether *FoxM1* was preferentially expressed in Sca-1$^+$ type II cells, real-time RT-PCR analysis of Sca-1$^+$ and Sca-1$^-$ type II cells isolated at 72 h after PA showed that the Sca-1$^+$ subpopulation of type II cells expressed greater *FoxM1* transcript than the Sca-1$^-$ type II cells (Fig. 3 G). Thus, FoxM1 was preferentially expressed in the activated subpopulation of type II cells, and timing of its expression was coincident with its postulated role in the mechanism of alveolar epithelial barrier repair.

Type II cell–specific deletion of *FoxM1* in mice

To address the role of FoxM1 expressed in type II cells in mediating alveolar epithelial barrier repair, we used *SPC-rtTA/TetO-Cre/FOXM1EKO* mouse line to disrupt the *FoxM1* gene specifically in type II cells. Expression of Cre recombinase is activated in alveolar type II cells by the doxycycline-inducible *rtTA/TetO* system coupled with type II cell–specific promoter *SPC* (Perl et al., 2002; Kalin et al., 2008). Cre mediates disruption of *FoxM1* in type II cells through the *loxP* sites flanking exons 4–7 of the *FoxM1* gene that encode the DNA binding and transcriptional activation domains (Fig. 4 A; Kalin et al., 2008). This doxycycline-inducible system enabled selective disruption of *FoxM1* in type II cells of adult lungs.

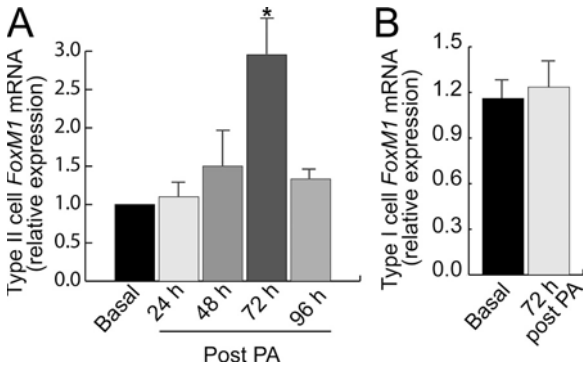

Figure 2. Time course of *FoxM1* expression in PA-challenged lungs. (A and B) Expression of *FoxM1* mRNA was evaluated by real-time RT-PCR in type I (B) and type II (A) cells before (basal) or at the indicted times after PA infection. Data are presented as mean ± SE (n = 3–5 mice for each group from three independent experiments; *, P < 0.05 vs. control).

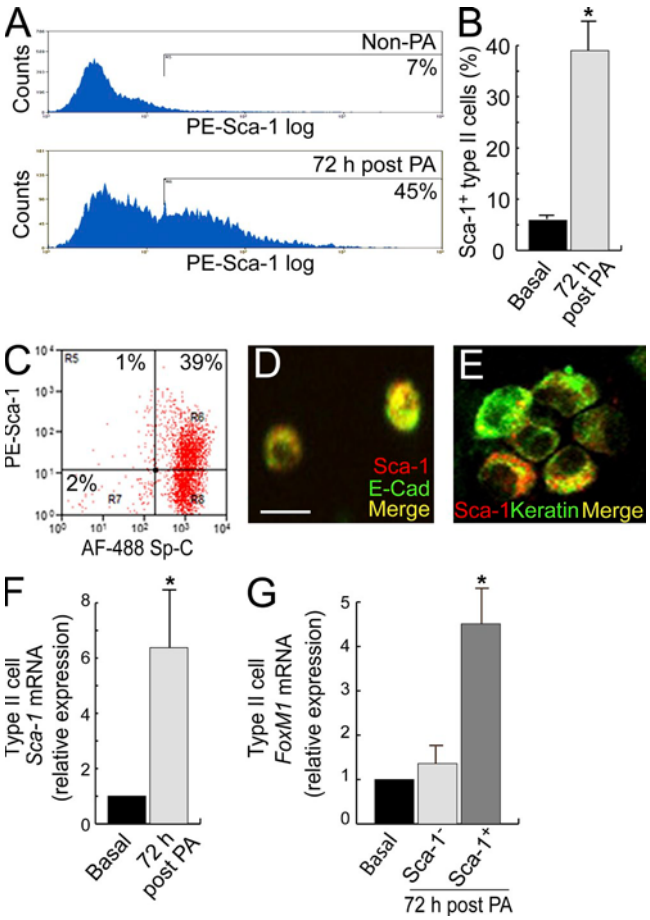

Figure 3. *FoxM1* transcript is enriched in Sca-1$^+$ type II cells early during the repair phase. (A) FACS analyses show the percentage of Sca-1$^+$ cells among type II cells before (non-PA) or 72 h after PA infection. Data are representative of more than five similar independent observations. (B) Percentage of Sca-1$^+$ cells in type II cells before and after PA challenge. Data are presented as mean ± SE (n = 9, more than five independent experiments; *, P < 0.05 vs. control). (C) FACS analysis showing Sca-1 and Sp-C expression on type II cells appearing at 72 h after PA infection. (A and C) Cells were gated on forward and side scatter to exclude debris and cell clusters. Numbers indicate the percentage of cells positive for the indicated marker out of total type II cells. (D and E) Expression of E-cadherin (E-Cad; D) and keratin (E) on Sca-1$^+$ type II cells. Bar, 10 µm. (C–E) Results are representative of three similar independent observations. (F) Relative expression of *Sca-1* mRNA in type II cells before (basal) or 72 h after PA infection as evaluated by real-time RT-PCR. (G) Relative expression level of *FoxM1* in Sca-1$^+$ and Sca-1$^-$ type II cells was evaluated by RT-PCR. (F and G) Data are presented as mean ± SE (n = 5 in three independent experiments; *, P < 0.05 vs. control).

Published June 27, 2011

The efficiency of inducible tissue-specific deletion was evaluated using the *SPC-rtTA/TetO-Cre/ROSA-YFP* mouse line (designated *ROSA-YFP*), in which the stop sequence flanked by two *loxP* sites is located at the *ROSA-YFP* locus to disrupt YFP expression. When Cre expression was induced through doxycycline, the stop sequence was deleted to enable YFP expression in type II cells as well as their progenies (Rawlins et al., 2009a). By antibody staining of lungs from mice fed doxycycline, we observed that >70% of the 800 Sp-C$^+$ cells from three mice were YFP$^+$, indicating a recombination frequency of 70% (Fig. 4, B–D). YFP expression in type II cells was doxycycline dependent because only 10% of type II cells expressed YFP in its absence (Fig. S3 A). In addition, >90% (total 420 cells from three mice; >100 cells from each mice were counted) of the cuboidal YFP$^+$ cells in alveoli were Sp-C$^+$ when mice were not challenged with PA (Fig. 4, B–D). In contrast, at 72 h after PA, YFP$^+$Sp-C$^-$ cuboidal cells were frequently observed (Fig. 4, E–G). Some of these cells were proliferating as shown by their BrdU labeling (Fig. S3, C and D), and some YFP$^+$Sp-C$^-$ cells expressed the type I cell marker T1α (Fig. S3, E and F). These results indicate that type II cells had lost their Sp-C expression and were actively engaged in repair at 72 h after PA challenge. In addition, we observed that at 72 h after PA, >70% of Sca-1$^+$ cells were YFP$^+$ (Fig. 4 H), which is consistent with the notion that these cells were derived from the Sp-C–expressing cells.

Mutant (*SPC-rtTA/TetO-Cre/FOXM1EKO*) mice were fed doxycycline for 2 wk to induce type II cell–specific disruption of *FoxM1*. Littermates with genotype *+/TetO-Cre/FOXM1EKO* were used as WT controls. In control mice lacking the *SPC-rtTA* transgene, Cre was not expressed and *FoxM1* was not disrupted. Mutant mice without PA challenge did not show any overt changes in behavior and lifespan. Type II cells were isolated and subjected to real-time RT-PCR analysis to assess messenger RNA (mRNA) expression of *FoxM1*. In noninfected lungs, *FoxM1* mRNA levels in mutant and WT cells were similar, which is likely the result of the 2–3-wk turnover rate of normal type II cells (Mason, 2006) and because *FoxM1* transcript is being produced before doxycycline administration. However, at 72 h after PA challenge, the amount of *FoxM1* mRNA in mutant type II cells was significantly lower than control (Fig. 4 I), indicating a marked disruption of *FoxM1* expression.

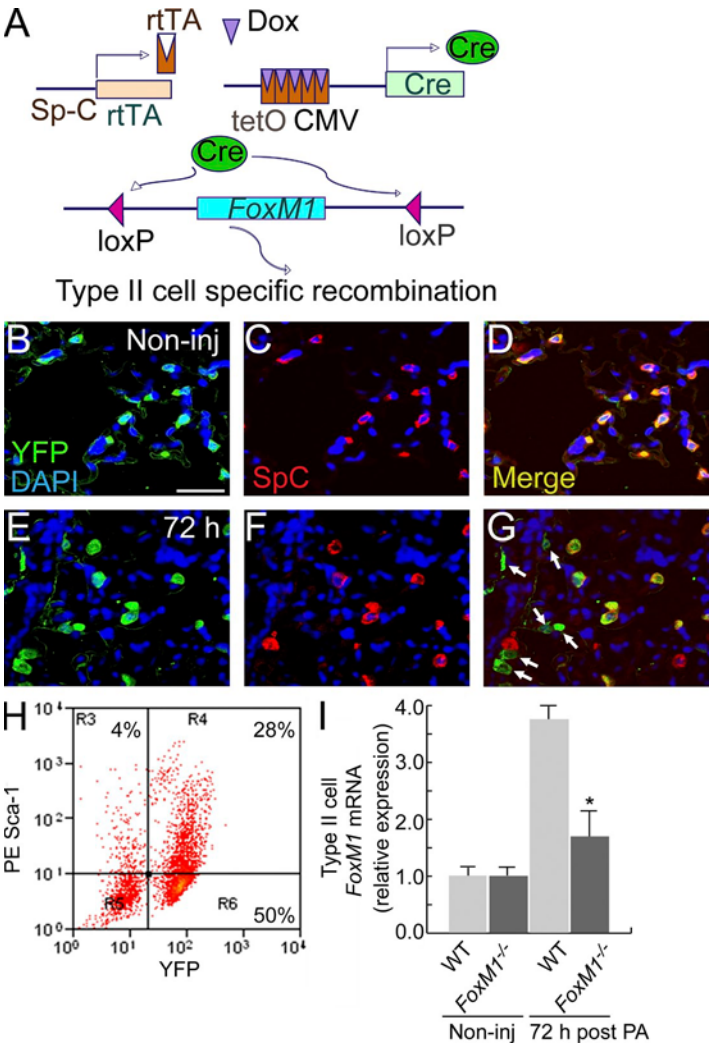

Decreased type II cell proliferation in *FoxM1* mutant lungs

We compared type II cell proliferation in control and mutant lungs by double labeling with antibodies to BrdU and Sp-C after PA-mediated injury. Lungs were isolated at 72 h after PA, and BrdU was injected at 5 h before lung isolation. We observed that the number of BrdU$^+$Sp-C$^+$ proliferating type II cells in mutant mice was significantly reduced even though the cells surrounding small blood vessels were proliferating at a similar rate as WT (Fig. 5, A–D).

Figure 4. Type II cell–specific disruption of *FoxM1* in mice. (A) An inducible type II cell–specific deletion system. rtTA protein is produced from type II cell–specific Sp-C promoter. After interacting with doxycycline, rtTA activates TetO-CMV promoter to produce Cre recombinase, which binds to the loxP sites and induces type II cell–specific recombination. (B–G) A *ROSA-YFP* line was used to show type II cell–specific recombination. Cells with Cre-induced recombination showed YFP expression. (B–D) *ROSA-YFP* lung without PA injection (Non-inj). The staining of YFP (B), Sp-C (C), and merge (D) are shown for the same section. (E–G) *ROSA-YFP* lung at 72 h after PA injection. The localization of YFP (E), Sp-C (F), and merge (G) are shown for one section. Note that some of the YFP$^+$ cuboidal cells are Sp-C$^-$ (arrows). Bar, 20 µm. (H) FACS analysis showing expression of Sca-1 and YFP in type II cells at 72 h after PA injection. Cells were gated on forward and side scatter to exclude debris and cell clusters. Numbers indicate the percentage of cells positive for the indicated marker out of total type II cells. Data are representative of three independent experiments. (I) Adult mice with genotype *SPC-rtTA/TetO-Cre/FOXM1EKO* or *+/TetO-Cre/FOXM1EKO* were fed with doxycycline for 2 wk, and lungs were then challenged with PA. *FoxM1* expression in type II cells before (Non-inj) or 72 h after PA challenge was assayed by real-time RT-PCR. Data are presented by mean ± SE (n = 3–5 mice for each group from three independent experiments; *, $P < 0.05$ vs. control).

Published June 27, 2011

For each mouse, we randomly selected 10 areas in the lung periphery to score proliferating type II cells. In control mice, 6.8 ± 0.9% of Sp-C$^+$ cells were BrdU$^+$, whereas only 2.7 ± 1.3% of Sp-C$^+$ cells in the mutant were BrdU$^+$ (mean ± SE; n = 3 mice; Fig. 5 E). Thus, *FoxM1* disruption in type II cells markedly reduced proliferation of these cells during the phase of alveolar repair after PA insult.

We also used the *SPC-rtTA/TetO-Cre/ROSA-YFP/FOXM1EKO* (*ROSA-YFP-EKO*) mouse line to compare cell proliferation in *FoxM1*$^+$ and *FoxM1*$^-$ type II cells of the same mouse lung. In this line, YFP$^+$ type II cells are expected to have Cre expression, and most of them have disrupted *FoxM1*, whereas most YFP$^-$ type II cells are without Cre and have WT *FoxM1*. Type II cells were isolated from *ROSA-YFP-EKO* mice and labeled with BrdU for 24 h. YFP$^+$ and YFP$^-$ cells were separated either by MoFlo fluorescent cell sorting or visually identified based on antibody staining against YFP. We found that 8% of YFP$^-$ cells were BrdU$^+$, whereas 4% of YFP$^+$ cells were BrdU$^+$ (Fig. 5 F). Thus, in the same lung, the proliferation rate of WT type II cells was double that of *FoxM1*-deleted type II cells.

CDC25C and cyclin B1, two critical factors required for cell cycle progression, are regulated by FoxM1 in endothelial cells (Zhao et al., 2006). To test their role in mediating type II cell proliferation, real-time RT-PCR analysis was performed in type II cells isolated at 72 h after infection. We observed that mRNA levels of both CDC25C and cyclin B1 were significantly decreased in *FoxM1*-deleted cells compared with control (Fig. 5, G and H). Thus, the decreased expression of CDC25C and cyclin B1 may contribute to the proliferation-defective phenotype of *FoxM1*-deficient type II cells seen during alveolar repair.

To determine whether overexpressing FoxM1 can drive type II cell proliferation, we infected cultured WT non–PA-treated type II cells with adenoviral vector expressing FoxM1 (Wang et al., 2002) or a control viral vector. When cultured with BrdU, FoxM1-expressing virus–infected cells show significantly greater BrdU incorporation than control cells (Fig. 5, I and J).

Defective type I cell trans-differentiation in *FoxM1*-deficient type II cells and impaired alveolar epithelial barrier recovery in mice

Because type II cells are believed to trans-differentiate into type I cells during alveolar repair

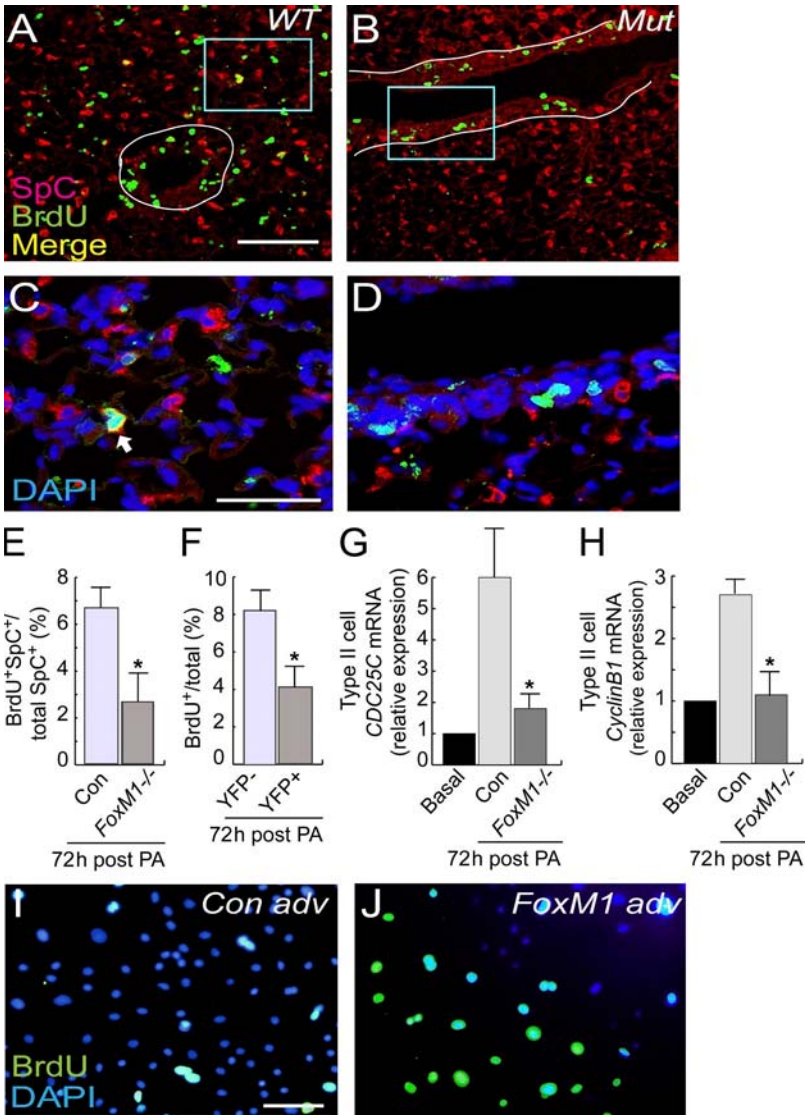

Figure 5. Defective type II cell proliferation in mouse lungs having *FoxM1* deleted in type II cells. (A and B) Double labeling of BrdU and Sp-C in WT (A) and mutant (Mut; *SPC-rtTA/TetO-Cre/FOXM1EKO*; B) lungs at 72 h after infection. Small blood vessels are indicated by thin white lines (B) or the circled area (A). (C and D) Higher magnification images of the blue rectangles in A and B, respectively. Arrow shows BrdU colocalization with Sp-C in a WT cell. Data are representative of three independent experiments. (E) Percentage of BrdU$^+$Sp-C$^+$ cells among Sp-C$^+$ cells in WT and mutant at 72 h after infection. (F) Type II cells were isolated from *ROSA-YFP-EKO* mice. YFP$^+$ and YFP$^-$ cells were separated and labeled with BrdU for 24 h. The percentage of BrdU$^+$ cells among YFP$^+$ (mutant) or YFP$^-$ (WT) type II cells were compared. (E and F) Data are presented as mean ± SE (*, $P < 0.05$ vs. control). 100–500 type II cells were scored in each sample (n = 3 mice for each group from three independent experiments). (G and H) Relative expression of CDC25C (G) and CyclinB1 (H) in uninfected WT cells (basal) and in WT (Con) and *FoxM1*$^{-/-}$ type II cells at 72 h after PA infection as assessed by real-time RT-PCR. Data are presented as mean ± SE (n = 3–4 mice for each group from three independent experiments; *, $P < 0.05$ vs. control). (I and J) Isolated WT, non–PA-treated type II cells cultured with BrdU were infected with control adenovirus (Con adv; I) or adenovirus expressing FoxM1 (FoxM1 adv; J). Data are representative of three independent experiments. Bars: (A and B) 60 µm; (C and D) 25 µm; (I and J) 20 µm.

Published June 27, 2011

(Evans et al., 1973, 1975), next we addressed whether disrupting *FoxM1* in type II cells resulted in a decreased number of type I cells and thereby led to impaired recovery of alveolar epithelial barrier function. First, we used *SPC-rtTA/TetO-Cre/ROSA-YFP/+* (*ROSA-YFP*) and *SPC-rtTA/TetO-Cre/ROSA-YFP/FOXM1EKO* (*ROSA-YFP-EKO*) mouse lines to follow the fate of YFP^+ cells after injury. In both lines, most (>90%; for each genotype, 300–400 cells from two to three mice were scored) of the cuboidal YFP^+ cells expressed the type II cell marker Sp-C in the absence of injury (Fig. 6, A, B, and I–J). At 5 d after infection, $YFP^+Sp\text{-}C^-$ cuboidal cells were frequently observed in *ROSA-YFP* lungs. Some of these cells formed clusters and expressed the type I cell marker T1α (Chen et al., 2004), and many of these cells were negative for type II cell marker Sp-C (Fig. 6, C–F). Many of these cells appeared to have higher YFP expression than the $Sp\text{-}C^+$ cells (Fig. 6, G and H), perhaps reflecting a higher metabolic rate of the activated type II cells than control cells. However, in *ROSA-YFP-EKO* lungs, we did not observe any cuboidal YFP^+ cell clusters, and most (>90%; three mice, 100–500 cells from each mouse were scored) of the YFP^+ cuboidal cells expressed Sp-C and not T1α (Fig. 6, K and L). Because in *ROSA-YFP-EKO* lungs *FoxM1*-mediated proliferation was disrupted only in type II cells, these findings demonstrate that the cuboidal $YFP^+Sp\text{-}C^-$ cell clusters observed in the control were derived from type II cells; thus, these cells were undergoing trans-differentiation into type I cells. Moreover, the mutant type II cells, although defective in proliferation, were also defective in type I cell trans-differentiation.

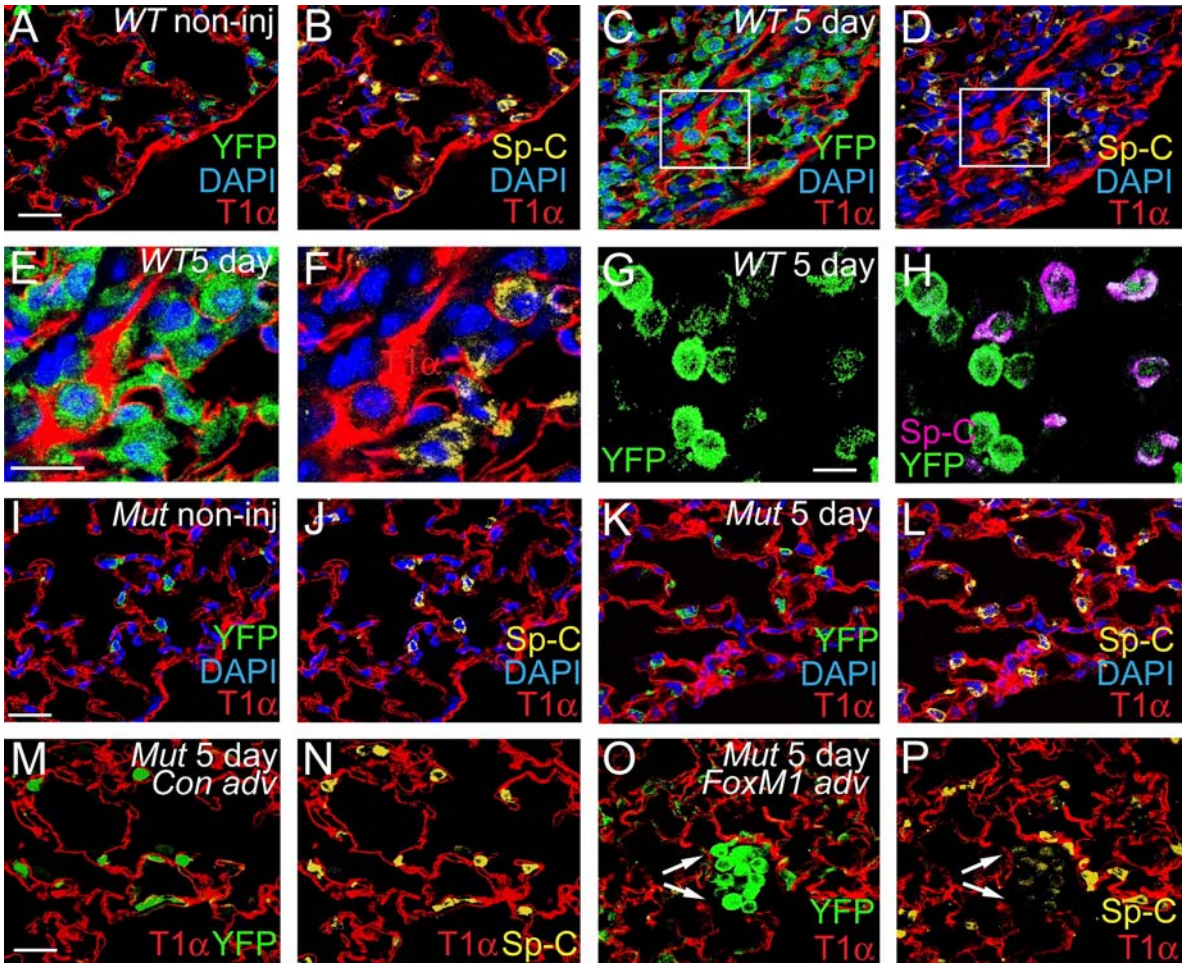

Figure 6. Defective activation and trans-differentiation of *FoxM1*-deficient type II cells in vivo. (A–L) WT (*ROSA-YFP*) and mutant (*ROSA-YFP-EKO*) lungs were compared in the noninfected (Non-inj; A, B, I, and J) and 5 d after PA infection groups (C–H, K, and L). (A–H) Lungs from control (*ROSA-YFP*) mice. (I–L) Lungs from mutant (*ROSA-YFP-EKO*) mice. A, C, I, and K were labeled with type I cell marker T1α and YFP, whereas B, D, J, and L are the same section as in A, C, I, and K, respectively, but labeled with T1α and type II cell marker Sp-C. E and F are higher magnifications of the areas in the white squares in C and D, respectively. G is the same section as in H, showing more examples of $YFP^+Sp\text{-}C^-$ cells in control lungs at 5 d after PA challenge. (M–P) Mutant (*ROSA-YFP-EKO*) lungs were infected with control virus (M and N) or adenovirus expressing FoxM1 (O and P). M and O were labeled with T1α and YFP, whereas N and P are the same section as in M and O, respectively, but labeled with T1α and Sp-C. Arrows denote clusters of cuboidal YFP^+ cells expressing faint Sp-C in the FoxM1 virus–infected lungs (O and P). Data are representative of three independent observations. Bars: (A–D and I–P) 20 µm; (E–H) 10 µm.

Published June 27, 2011

Next we determined whether expression of FoxM1 would induce type II cells to trans-differentiate into type I cell in the *FoxM1* mutant. We i.t. injected adenovirus expressing FoxM1 (Wang et al., 2002) in *YFP-EKO* mice. At 5 d after PA infection, the YFP^+ type II cell clusters frequently observed in FoxM1 adenovirus–injected lungs expressed significantly lower levels of Sp-C (Fig. 6, O and P), indicating partial trans-differentiation into type I cells. In contrast, in control virus–injected YFP-EKO lungs, no such clusters were observed; rather, the YFP^+ type II cells expressed high levels of Sp-C (Fig. 6, M and N). Thus, FoxM1 expression partially rescued the mutant phenotype of defective type II to type I cell trans-differentiation.

Next, we used an in vitro system using T1α and Aqp5 (aquaporin 5) as type I cell markers (Ma et al., 2000) to further address the mechanism of trans-differentiation of type II cells into type I cells. Type II cells were isolated at 72 h after infection from *ROSA-YFP* or *ROSA-YFP-EKO* lungs and cultured for ∼30 h. In *ROSA-YFP* culture, the majority of cells became flat type I–like cells and some expressed T1α, whereas the majority of *ROSA-YFP-EKO* type II cells remained cuboidal and did not express T1α (Fig. 7, A and B). To quantify the trans-differentiated cells, type II cells were isolated at 72 h after infection and processed for RT-PCR. We observed that both WT and mutant cells expressed similar levels of *Aqp5*. However, after these cells were cultured for ∼30 h, type II cells from control mice trans-differentiated into type I cells and expressed higher levels of Aqp5, whereas the mutant cells expressed low levels of Aqp5 (Fig. 7 C), indicating a defective trans-differentiation phenotype.

We have shown that β-catenin is a transcriptional target of FoxM1 (Mirza et al., 2010) and may play an important role in the type II to type I cell trans-differentiation (Flozak et al., 2010). Here we used real-time RT-PCR to examine the type II cell expression level of *β-catenin* during trans-differentiation in WT and *FoxM1* mutant type II cells. We observed that both WT and mutant type II cells expressed similar levels of *β-catenin* before and at 72 h after PA. However, when the cells from the PA-infected lung were cultured for ∼30 h to induce trans-differentiation, the expression of *β-catenin* in the mutant was significantly lower than control (Fig. 7 D), suggesting that β-catenin is a candidate downstream target of FoxM1 regulating type II to type I cell trans-differentiation.

To assess injury and repair of the alveolar barrier, bronchoalveolar lavage (BAL) fluid was collected at 48 h, 96 h, and 5 d after PA injection. At 48 h, BAL protein concentration was elevated in both control and mutant, indicating that the degree of alveolar barrier leakiness was similar. At 96 h to 5 d, the protein concentrations returned to basal level in control lungs but remained high in the mutant (Fig. 8 A), indicating that the barrier function was largely restored in WT but remained defective in mutant lungs. We next examined the cells in BAL. At 48 h, total cell counts in both control and mutant sample were high (Fig. 8 B). Hema3 staining showed that most of these cells were neutrophils (unpublished data), indicating increased inflammatory cell influx. At 96 h, the cell numbers were reduced to basal level in control but remained high in mutant lungs (Fig. 8 B). Hema3 staining showed that most cells in control BAL were macrophages, whereas mostly neutrophils were present in BAL from the mutant lungs (Fig. 8, C and D). Thus, the initial

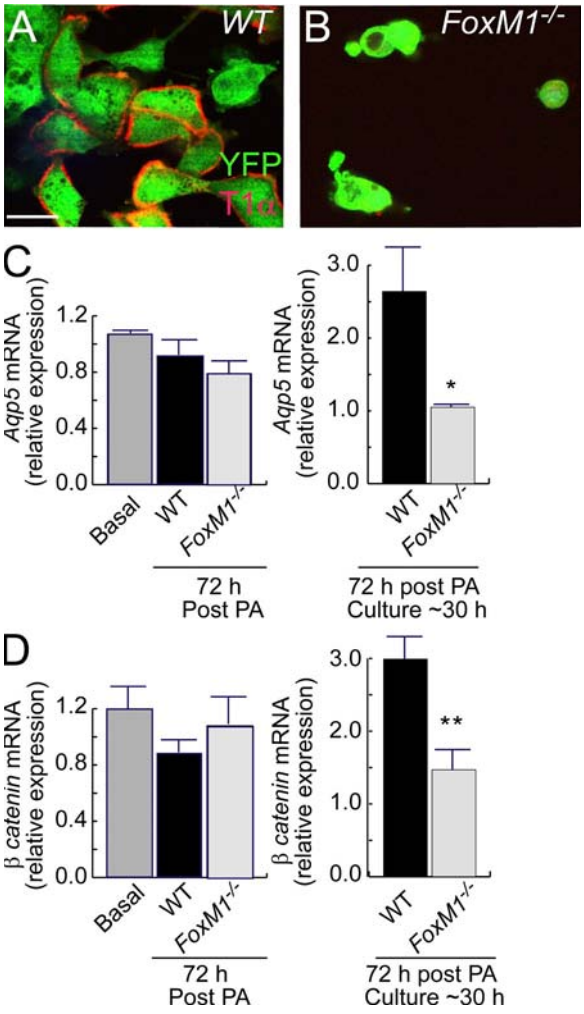

Figure 7. Defective trans-differentiation of *FoxM1*-deficient type II cells into type I cells in vitro. (A and B) Type II cells were isolated from WT (*ROSA-YFP*; A) and mutant (*ROSA-YFP-EKO*; B) lungs at 72 h after PA injection and cultured for ∼30 h (24–36 h) to allow trans-differentiation into type I cells. Cells were stained with antibody specific for T1α. Data are representative of three independent observations. Bar, 10 µm. (C and D) Type II cells were isolated in non–PA-injected lungs (basal) as well as in lungs 72 h after PA injection of WT (*+/TetO-Cre/FOXM1EKO*) and mutant (*SPC-rtTA/TetO-Cre/FOXM1EKO*) mice, and the relative expression of mRNA encoding the type I cell marker *Aqp5* (C) and *β-catenin* (D) was measured by real-time RT-PCR. In another experiment, type II cells were isolated from WT (*+/TetO-Cre/FOXM1EKO*) and mutant (*SPC-rtTA/TetO-Cre/FOXM1EKO*) lungs at 72 h after PA injection and cultured for ∼30 h (24–36 h) to allow trans-differentiation into type I cells. RNA was then isolated from cultured cells for real-time RT-PCR analysis of *Aqp5* (C) and *β-catenin* (D) mRNA. Data are presented by mean ± SE (n = 3–5 mice for each group from three independent experiments; *, $P < 0.05$ vs. control; **, $P = 0.01$ vs. control).

Published June 27, 2011

responses were similar in WT and mutant lungs, whereas mutant lungs showed a prolonged inflammatory response indicating an impaired recovery.

Similar initial inflammatory response in *FoxM1* mutant and WT lungs induced by PA

Fig. 9 A shows that changes of MIP2 (macrophage inflammatory protein 2) generation, a major cytokine involved in attracting neutrophils (Kobayashi, 2008), during the course of injury and repair were similar in both WT and mutant lungs; both showed high concentrations of MIP2 at 48 h after PA and returned to basal levels at 96 h. We cultured lung lysates to examine bacterial colony growth because this could account for different rates of recovery. In both control and mutant, we did not observe growing bacteria colonies at 48 h after infection (n = 3 mice for each group from three independent experiments), indicating that bacteria were cleared from lungs with similar efficiency in both groups.

Sp-A, Sp-B, and Sp-D are SAPs reported to be downstream targets of FoxM1 during fetal lung development (Kalin et al., 2008). Sp-A and Sp-D play a role in modulating pulmonary innate immunity by interacting with pathogen-derived components and macrophages (Sano and Kuroki, 2005). Sp-A– or Sp-D–null mice manifested delayed microbial clearance and overexpression of proinflammatory cytokines (Sano and Kuroki, 2005). We observed by Western blot analysis that both Sp-A and Sp-D were expressed similarly in mutant and control lungs at 96 h after infection (Fig. 9, B and C). Measurement of the amount of these two proteins (quantified by measuring their signal intensity and normalized to β-actin expression) showed that the relative expression of Sp-A was 1.1 ± 0.3 in control and 0.8 ± 0.2 in the mutant. Relative expression of Sp-D was 0.5 ± 0.2 in control and 0.6 ± 0.2 in mutant (mean ± SE; n = 3 mice for each group from three independent experiments). Thus, expression of Sp-A and Sp-D in mutant lungs was the same range as control. Furthermore, expression of Sp-B also did not show a significant difference between control and mutant (Fig. 9 D), indicating that the severity of injury and initial immune response in mutant lungs were similar to control. Thus, the prolonged alveolar barrier defect of mutant lungs is likely the result of a defective repair program secondary to deletion of *FoxM1* rather than any difference in the severity of injury or inflammation.

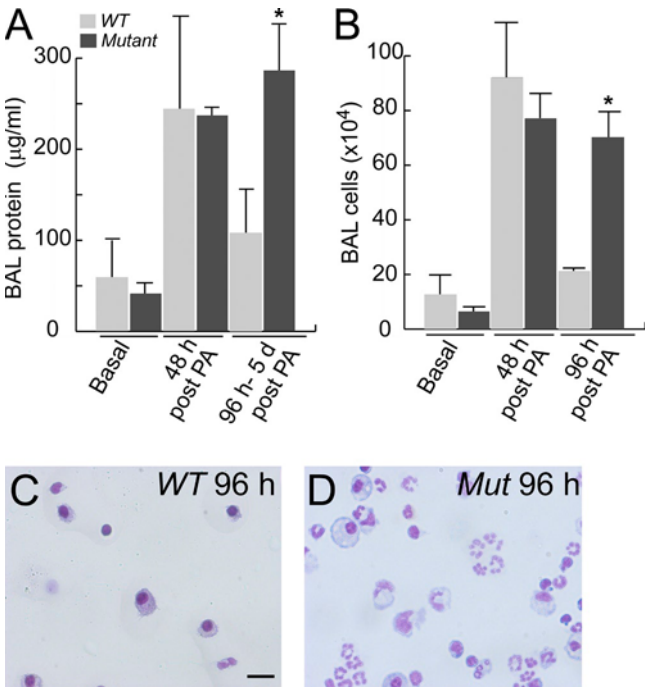

Figure 8. Failure of alveolar barrier repair after PA challenge in lungs with *FoxM1* deleted in type II cells. (A and B) Protein concentration and cell number in BAL isolated from WT and mutant (*SPC-rtTA/TetO-Cre/FOXM1EKO*) lungs. At 48 h and 96 h to 5 d after infection, protein concentrations (A) and cells (B) were measured in both samples. Data are from at least three independent experiments and are presented as mean ± SE (n = 3 mice for each group in B; n = 3 mice for each group for 0 h and 48 h in A). At 96 h to 5 d, the data were collected in three WT and three mutants at 96 h and two for each group at day 5 (*, $P < 0.05$ vs. control). (C and D) At 96 h after infection, cells from control (C) and mutant (D) lungs were analyzed to distinguish monocytes and neutrophils. Data are representative of three independent observations. Bar, 20 μm.

DISCUSSION

We have identified in this study the fundamental importance of the transcription factor FoxM1 expressed in alveolar type II cells in the mechanism of alveolar epithelial barrier repair after PA-induced lung injury. We used PA because it induces alveolar injury similar to that encountered in pneumonia (Gray and Kreger, 1979; Sadikot et al., 2006). We showed that type II cell–specific disruption of *FoxM1* markedly delayed the recovery of alveolar barrier function as indicated by prolonged neutrophil influx and increased BAL protein concentration. There was a persistent alveolar barrier defect in *FoxM1*

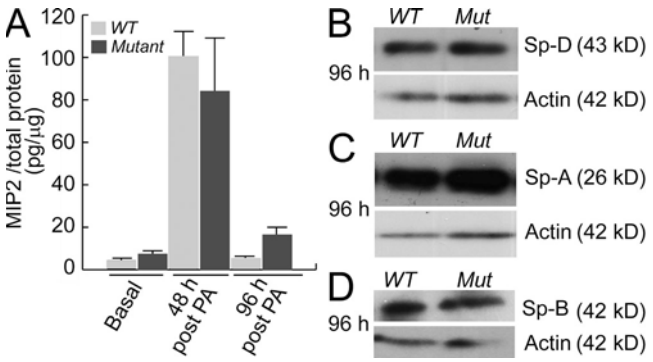

Figure 9. Similar inflammatory response of the *FoxM1* mutant and control lungs. (A) MIP2 concentrations in WT and mutant (*SPC-rtTA/TetO-Cre/FOXM1EKO*) lung lysates before (basal) and 48–96 h after PA infection. Data are presented as mean ± SE (n = 3 mice for each group from three independent experiments). (B–D) Protein expression of Sp-D (B), Sp-A (C), and Sp-B (D) in WT and mutant (Mut) lungs at 96 h after PA infection as assessed by Western blot analysis. Data are representative of three independent observations.

Published June 27, 2011

mutants caused by defective type II cell proliferation and trans-differentiation into type I cells.

Although type I cells comprise ∼95% of the alveolar surface area, studies have shown that type II cells mediate the regeneration of type I alveolar cells and restoration of barrier function after alveolar injury (Evans et al., 1973, 1975). Type II cells after injury thus function as progenitor cells because they can self-renew and trans-differentiate into type I cells (Evans et al., 1973, 1975; Mason, 2006; Sugahara et al., 2006). This specialized function of type II cells has been proposed to play a fundamental role in alveolar epithelial barrier repair (Rawlins and Hogan, 2006; Stripp, 2008). We focused in this study on the role of the transcription factor FoxM1 in regulating the progenitor function of type II cells. FoxM1 expression was increased in type II cells only during the repair phase after PA injury. In contrast, expression of *FoxM1* in type I cells did not increase during this period, suggesting that *FoxM1* in type I cells does not participate in the repair. We observed that *FoxM1* mutant type II cells had greatly reduced proliferation rates and severely impaired trans-differentiation into type I cells, resulting in a failed alveolar barrier repair program. These results provide the first evidence to our knowledge of the essential role of FoxM1 in type II cells in the mechanism of alveolar barrier repair.

Although the alveolar barrier defect observed in *FoxM1* mutant lungs indicates a defective repair, an alternative explanation could be an enhanced inflammatory response in the mutant lungs. However, this is unlikely because the postinjury changes in MIP2 concentration, a marker of inflammation, were similar in *FoxM1* mutant and WT lungs. The mutant lungs also cleared bacteria as rapidly as WT, thus precluding any differences in bacterial clearance and resulting lung inflammation as the basis for delayed alveolar epithelial barrier recovery seen in *FoxM1* mutant lungs. A previous study showed that FoxM1 can regulate the expression of SAPs during embryogenesis (Kalin et al., 2008). The SAPs Sp-A and Sp-D in particular play a role in the lung's immune response (Sano and Kuroki, 2005). However, we observed that the mutant lungs exhibited the same levels of these proteins as WT, ruling out the role of SAPs in the delayed epithelial barrier recovery response seen in *FoxM1* mutant lungs.

Type II cell proliferation was increased in WT but not in *FoxM1*-deleted mice, indicating that FoxM1 was required for type II cell proliferation during repair. FoxM1 has been shown to regulate the expression of proteins involved in cell cycle progression (Costa et al., 2005). We observed that CDC25C and cyclin B1 were the likely FoxM1 downstream targets responsible for type II cell–mediated proliferation. A study has shown that *FoxM1* disruption in the embryonic lung epithelium did not affect the proliferation of alveolar precursor cells (Kalin et al., 2008), suggesting that FoxM1 does not play a role in mediating cell proliferation during lung development. However, in our study, we used an inducible system in which the *FoxM1* gene was deleted in adult type II cells before induction of lung injury, thus bypassing the known effects of FoxM1 in embryonic development.

The *FoxM1* mutant type II cells also showed defective trans-differentiation into type I cells in both in vitro and in vivo experiments. We surmised from this observation that FoxM1 regulates expression of genes involved in the formation of type I cells. Our results suggested that *β-catenin* is a candidate target of FoxM1 regulating the type II to type I cell trans-differentiation, which is consistent with the evidence that FoxM1 binds to the promoter of *β-catenin* and directly regulates *β-catenin* expression (Mirza et al., 2010). β-catenin is also involved in the mechanism of differentiation of various cell types including lung cells (Mucenski et al., 2005; De Langhe and Reynolds, 2008; Grigoryan et al., 2008) and has been shown to play a key role in the type II to type I cell trans-differentiation (Flozak et al., 2010). Our result suggest that FoxM1 interacts with the Wnt/catenin signaling (Grigoryan et al., 2008) in regulation of type II to I cell trans-differentiation after injury.

Notably, FoxM1 expression in type II cells increased only during the early repair phase when a subpopulation of cells adopted a progenitor phenotype as indicated by their co-expression of Sca-1. Given that Sca-1 is a marker of progenitor cells (Holmes and Stanford, 2007), these findings suggest that Sca-1$^+$FoxM1$^+$ type II cells represent the pool of regenerating type II cells. We found that Sca-1$^+$ type II cells had a higher potential of trans-differentiation into type I cells in vitro than the Sca-1$^-$ counterpart (unpublished data). However, it is not clear whether the Sca-1$^+$ type II cells appearing after PA are derived from expansion of an existing Sca-1$^+$ population or from reprogramming of quiescent Sca-1$^-$ type II cells. We found that in the type II cell–specific *FoxM1* mutant mouse, although *FoxM1*$^{-/-}$ type II cells showed impaired cell proliferation, these mutant lungs generated a relatively high ratio of Sca-1$^+$ type II cells at 72 h after PA (40 ± 8% Sca-1$^+$ among total type II cells; $n = 4$ mice in two independent experiments), similar as WT lungs. Thus, it is unlikely that the Sca-1$^+$ cells appearing at 72 h after PA are derived from an expansion of preexisting Sca-1$^+$ cells. Furthermore, the percentage of Sca-1$^+$ type II cells in the total type II cell population can be as much as 60% after injury, further supporting the claim that they are derived from the reprogramming of quiescent Sca-1$^-$ type II cells. Some previous studies have also suggested a heterogeneity among type II cells; e.g., some type II cells expressed a lower level of E-cadherin than others (Reddy et al., 2004), whereas others expressed a relatively low level of CC10 (Kim et al., 2005b; Rawlins et al., 2009a). Thus, the type II cell subpopulation expressing higher amounts of both FoxM1 and Sca-1 may serve as progenitor cells responsible for the proliferation and trans-differentiation of type II cells needed to regenerate the alveolar epithelial barrier after PA injury.

One might expect that adult type II cells after injury revert to a state resembling alveolar precursor cells during embryogenesis; however, we did not see any differences in expression of several transcription factors, *Id2*, *Erm*, *Gata6*, and *Elf5*, involved in alveolar development (Liu et al., 2003; Metzger et al., 2008; Zhang et al., 2008; Rawlins et al., 2009b).

Published June 27, 2011

Furthermore, FoxM1 was not required for proliferation of the embryonic lung epithelium (Kalin et al., 2008), whereas, as we have shown in this study, it is required for proliferation of adult type II cells during repair. Thus, the mechanism of trans-differentiation of type II to type I cells during alveolar repair is different from differentiation from alveolar precursor cells into type II and I cells during embryogenesis.

In conclusion, we have identified FoxM1 in type II alveolar epithelial cells as the key regulator of alveolar epithelial barrier repair through its ability to control proliferation and trans-differentiation into type I cells. As FoxM1 is the first transcription factor shown to regulate alveolar barrier repair, these findings raise the possibility of pharmacologically targeting FoxM1 in type II cells to restore alveolar homeostasis after lung inflammatory injury in diseases such as acute respiratory distress syndrome.

MATERIALS AND METHODS

Mice stain and PA injury model. The animal experiments were approved by the Animal Care Committee and Institutional Biosafety Committee of the University of Illinois at Chicago. The *SPC-rtTA/TetO-Cre/FOXM1EKO* mouse line, which carries transgenes for *SPC-rtTA* and *TetO-Cre*, is homozygous for the *FoxM1loxP* locus and is in C57/FVB mixed genetic background (Kalin et al., 2008). This line was used for doxycycline-induced type II alveolar cell–specific deletion of the *FoxM1* gene. In our study, mutant genotype refers to *SPC-rtTA/TetO-Cre/FOXM1EKO*, whereas control genotype refers to *+/TetO-Cre/FOXM1EKO*. Mice were fed with 1 mg/ml doxycycline in drinking water for 14 d and then in normal water for 1 wk before experiments. Each experiment was made with paired litter mates of mutant and control genotype of the same gender.

B6.129X1-Gt(ROSA)26Sortm1(EYFP)Cos/J mice were obtained from the Jackson Laboratory and were crossed with *SPC-rtTA/TetO-Cre/FOXM1EKO* mice to generate *SPC-rtTA/TetO-Cre/ROSA26-YFP/+* and *SPC-rtTA/TetO-Cre/ROSA26-YFP/FOXM1EKO* mice. All mice were fed with doxycycline unless specified otherwise in the text.

PA (strain 103) was prepared as described previously (Sadikot et al., 2006). Mice were challenged with 5×10^6 CFU PA via i.t. instillation.

Isolation and culture of type II cells. Type II cells were isolated as described previously (Rice et al., 2002; Gobran and Rooney, 2004). In brief, the lung was first perfused by 10 ml PBS through the right ventricle to wash out the blood, and then 2 ml Dispase (BD) was injected i.t. and followed by 0.5 ml melted agarose (45°C). The cells were dissociated by Dispase and DNase I treatment and panned by tissue culture plates coated with anti-CD45 and anti-CD32 antibodies. The cells were then collected by centrifugation at 150 *g* for 6 min. The purity of type II cells was accessed by a modified Papanicolaou stain (Dobbs, 1990), and only preps with >90% purity were used for subsequent experiments.

To access the trans-differentiation into type I cells, type II cells were isolated and cultured in tissue culture–treated plates (Corning). The cells were grown in DME with 15 mM Hepes, 10% FBS, penicillin/streptomycin, and glutamine for 24–48 h, and the cultured cells were processed for RNA isolation or antibody staining.

Isolation of type I cells. Type I cells were isolated by elastase digestion as described previously (Chen et al., 2004; Gonzalez et al., 2009). Lungs were perfused through the pulmonary artery with PBS. 2 ml of solution D (RPMI 1640 medium with 25 mM Hepes, pH 7.2) containing 10% dextran 40 and 4.5 U/ml elastase (Worthington) was instilled i.t., and the lung was incubated at 37°C for 30 min. Cells were subsequently dissociated in solution D with 20% FBS and 100 U/ml DNase I (Sigma-Aldrich) and centrifuged for 15 min at 250 *g*. Cells were then stained with hamster anti-T1α antibody (Developmental Studies Hybridoma Bank) and Cy3 or Cy5 secondary antibody (Jackson ImmunoResearch Laboratories, Inc.). $T1\alpha^+$ cells were isolated by MoFlo high speed cell sorting performed at the Flow Cytometry Core at the University of Illinois at Chicago.

Real-time PCR. RNA was extracted by TRIZOL (Invitrogen), treated by DNase I (QIAGEN), and purified with an RNeasy kit (QIAGEN). Real-time RT-PCR was performed using a Quanti-Tect SYBR Green RT-PCR kit (QIAGEN) and ABI Prism 7000 Sequence Detection System (Applied Biosystems). Primers are listed in Table S1; the primers for CDC25C, Cyclin B1, and β-catenin were obtained from QIAGEN. Data were analyzed using the comparative Cτ method. Relative quantification to the control sample calibrator was calculated using the formula $2^{-(\Delta\Delta C\tau)}$. Gene expression was normalized to the level of cyclophilin (*CLO*) as an internal control (Zhao et al., 2002).

Flow cytometry. For fluorescent cell sorting of Sca-1^+ and Sca-1^- cells, freshly isolated type II cells were resuspended to $\sim 1.0 \times 10^6$ cell/ml in cold PBS/2% BSA, stained with PE- or APC-labeled rat anti–Sca-1 mAb as well as PE or APC-rat IgG2a isotype control (eBioscience) at 0.25 μg antibody per million cells for 50 min and washed by PBS/2% BSA. The cells were sorted with the MoFlo high speed cell sorter (BD) at the Flow Cytometry Service Core at the University of Illinois at Chicago. Cells were gated on forward and side scatter to exclude debris and cell clusters. Reanalysis of fluorescent profile after the sort showed that the purity of sorting is ~99%. For sorting of YFP^+ and YFP^- cells, freshly isolate type II cells were directly sorted with the MoFlo high speed cell sorter without staining.

For FACS phenotyping, freshly isolated type II cells were unfixed or fixed with 4% paraformaldehyde for 15 min at room temperature and permeabilized with 0.1% Triton X-100 in PBS for 10 min, and the treated cells were processed for antibody staining. For all experiments, isotype control and single color control were performed. The stained cells were sorted using a CyAn ADP flow cytometer (Beckman Coulter) located at the Flow Cytometry Service Core. The results were analyzed with Cytomation Summit 4.3 software.

Immunohistochemistry. The blood in lungs was washed out by perfusion with 10 ml PBS through the right ventricle. The lung was then inflated with 2 ml of 4% paraformaldehyde/PBS i.t. and fixed in this solution at 4°C overnight before proceeding to paraffin embedding and sectioning at the Histology Core at the University of Illinois at Chicago. Hematoxylin and eosin (H&E) staining was also performed at the Histology Core. For preparing frozen sections, the lung was injected with 2 ml of 80% OCT/PBS i.t. and embedded in 100% OCT (Tissue Tek) and then quickly frozen in −70°C. 7-μm sections were cut using a cryostat. In some experiments, freshly isolated type II cells were immobilized on Superfrost/Plus microscope slides (Thermo Fisher Scientific) by cytospin centrifugation and fixed with 4% paraformaldehyde/PBS for 30 min at room temperature.

For BrdU labeling, the mice were injected with BrdU (75 mg/kg body weight) by i.p. injection at 5 h before tissue collection unless otherwise specified in the Results section. Tissue was treated with citrate antigen unmask solution (Vector Laboratories) for 10 min at 95°C before proceeding to anti-BrdU antibody staining. TUNEL (terminal deoxynucleotidyl transferase dUTP-biotin nick end labeling) assay was performed using the fluorescein in situ cell death detection kit (Roche) on frozen lung sections.

The following antibodies were used in this study: anti-BrdU (BD) was used at 1:3, anti–Sp-C (Millipore) was used at 1:1,000, and anti-GFP antibody (Aves Laboratories) was used at 1:500 for detecting YFP. The background for each ROSA-YFP mouse varied, but the signal of YFP^+ type II cells was robust compared with background. mAb to T1α (used at 1:20) was obtained from the Developmental Studies Hybridoma Bank. Fluorescent secondary antibodies (Cy3, Alexa Fluor 488, or Cy5; Jackson ImmunoResearch Laboratories, Inc. or Invitrogen) were used at 1:200. Images were captured by a confocal microscope (LSM 510; Carl Zeiss) located at the Imaging Core Facility at the Department of Pharmacology (University of Illinois

Published June 27, 2011

at Chicago). The images were captured at room temperature using a 63× NA 1.2 objective lens mediated by water, except in Figs. S1 (A and B) and S3 (A and B), in which 20× lenses were used to show more cells in one image window. The images were captured and processed using LSM 510 software (Carl Zeiss). Single images were acquired, and no operations such as deconvolution, 3D reconstitutions, or surface or volume rendering were performed. Fig. S1 (D and E) was captured using a 10× lens and an imaging system (Axioplan-2; Carl Zeiss). Fig. 5 (I and J) was captured using a 20× lens and an Axioplan-2 imaging system.

Adenovirus production and infection. A replication-defective E1- and E3-negative adenovirus expressing human FoxM1B, AdFoxM1, was constructed as described previously using standard overlap recombination (Wang et al., 2002). This recombinant virus was twice plaque purified, and adenovirus particles were purified from 293 cell lysate by CsCl centrifugation and dialyzed to remove the CsCl as described previously (Wang et al., 2002). The second recombinant virus, AdFoxM1B-TA, lacks the terminal 60 aa (689–748), which coincide with the transcriptional activation domain of the protein and the protein encoded fails to activate a transcriptional reporter fused to 6 multimers of the FoxM1/FoxA binding motif (Wierstra and Alves, 2006). The recombinant virus, AdHCMVap1LacZ, containing the β-galactosidase reporter gene, was a gift from F. Graham (McMaster University, Hamilton, Ontario, Canada; Graham and van der Eb, 1973). AdFoxM1B-TA or AdHCMVap1LacZ was used as control. For infection of cultured type II cells, the adenovirus particles were incubated with cells in serum-free media for 40 min at room temperature, with a multiplicity of infection of 20. For in vivo infection of the virus in lungs, $\sim 5 \times 10^8$ PFU virus in PBS were injected i.t. at 3 d before PA injection.

BAL analysis. BAL fluid was collected as described previously (Sadikot et al., 2006). Approximately 1 ml BAL was collected for each mouse, and protein concentration was determined using the Micro BCA protein assay kit (Thermo Fisher Scientific). Cells in BAL were quantified using a hemocytometer. Cells were immobilized on Superfrost/Plus microscope slides by cytospin centrifugation and further stained using a Hema3 staining kit as described previously (Sadikot et al., 2006).

Western analysis and cytokine quantification. Lung lysates were collected as described previously (Zhao et al., 2006), and protein concentration was determined using the Micro BCA protein assay kit. 50 μg of total protein was loaded in each lane for Western blot analysis. The following primary antibodies were used: anti–Sp-A, anti–Sp-B, and anti–Sp-D (Millipore) at 1:1,000. Antiactin (Santa Cruz Biotechnology, Inc.) was used as loading control. Protein quantification was further determined by measuring the intensity of the signal in Western blot films using the ImageJ program (National Institutes of Health).

MIP2 levels in lung lysates were measured using the Quantikine mouse CXCL2/MIP2 Immunoassay kit (R&D Systems). 25 μl of lysates was used for each sample, and the concentration of cytokines was normalized to the total protein amount.

Statistics. Differences between groups were examined for statistical significance using the Student's *t* test. $P < 0.05$ denoted the presence of a statistically significant difference.

Online supplemental material. Fig. S1 shows additional analysis of the PA lung injury model. Fig. S2 shows the expression level of several genes in type II cells from PA-challenged lungs. Fig. S3 shows additional analysis of the *SPC-rtTA/TetO-Cre/ROSA-YFP/+* (*ROSA-YFP*) mouse line. Table S1 shows the sequences of the primers for RT-PCR used in this study. Online supplemental material is available at http://www.jem.org/cgi/content/full/jem.20102041/DC1.

We thank the Flow Cytometry Service Core at the University of Illinois at Chicago for performing the MoFLo sorting and assistance in FACS analysis. We thank Dr. Brigid Hogan for discussion and insights.

This work was supported by National Institutes of Health grants HL07829-16 and HL090152.

The authors have no conflicting financial interests.

Submitted: 27 September 2010
Accepted: 25 May 2011

REFERENCES

Barker, N., and H. Clevers. 2007. Tracking down the stem cells of the intestine: strategies to identify adult stem cells. *Gastroenterology*. 133:1755–1760. doi:10.1053/j.gastro.2007.10.029

Blanpain, C., W.E. Lowry, A. Geoghegan, L. Polak, and E. Fuchs. 2004. Self-renewal, multipotency, and the existence of two cell populations within an epithelial stem cell niche. *Cell*. 118:635–648. doi:10.1016/j.cell.2004.08.012

Chen, J., Z. Chen, T. Narasaraju, N. Jin, and L. Liu. 2004. Isolation of highly pure alveolar epithelial type I and type II cells from rat lungs. *Lab. Invest.* 84:727–735. doi:10.1038/labinvest.3700095

Costa, R.H., V.V. Kalinichenko, M.L. Major, and P. Raychaudhuri. 2005. New and unexpected: forkhead meets ARF. *Curr. Opin. Genet. Dev.* 15:42–48. doi:10.1016/j.gde.2004.12.007

De Langhe, S.P., and S.D. Reynolds. 2008. Wnt signaling in lung organogenesis. *Organogenesis*. 4:100–108. doi:10.4161/org.4.2.5856

Dobbs, L.G. 1990. Isolation and culture of alveolar type II cells. *Am. J. Physiol.* 258:L134–L147.

Dor, Y., J. Brown, O.I. Martinez, and D.A. Melton. 2004. Adult pancreatic beta-cells are formed by self-duplication rather than stem-cell differentiation. *Nature*. 429:41–46. doi:10.1038/nature02520

Erker, L., and M. Grompe. 2008. Signaling networks in hepatic oval cell activation. *Stem Cell Res. (Amst.)*. 1:90–102. doi:10.1016/j.scr.2008.01.002

Evans, M.J., L.J. Cabral, R.J. Stephens, and G. Freeman. 1973. Renewal of alveolar epithelium in the rat following exposure to NO2. *Am. J. Pathol.* 70:175–198.

Evans, M.J., L.J. Cabral, R.J. Stephens, and G. Freeman. 1975. Transformation of alveolar type 2 cells to type 1 cells following exposure to NO2. *Exp. Mol. Pathol.* 22:142–150. doi:10.1016/0014-4800(75)90059-3

Flozak, A.S., A.P. Lam, S. Russell, M. Jain, O.N. Peled, K.A. Sheppard, R. Beri, G.M. Mutlu, G.R. Budinger, and C.J. Gottardi. 2010. Beta-catenin/T-cell factor signaling is activated during lung injury and promotes the survival and migration of alveolar epithelial cells. *J. Biol. Chem.* 285:3157–3167. doi:10.1074/jbc.M109.070326

Gobran, L.I., and S.A. Rooney. 2004. Pulmonary surfactant secretion in briefly cultured mouse type II cells. *Am. J. Physiol. Lung Cell. Mol. Physiol.* 286:L331–L336. doi:10.1152/ajplung.00334.2003

Gonzalez, R.F., L. Allen, and L.G. Dobbs. 2009. Rat alveolar type I cells proliferate, express OCT-4, and exhibit phenotypic plasticity in vitro. *Am. J. Physiol. Lung Cell. Mol. Physiol.* 297:L1045–L1055. doi:10.1152/ajplung.90389.2008

Graham, F.L., and A.J. van der Eb. 1973. A new technique for the assay of infectivity of human adenovirus 5 DNA. *Virology*. 52:456–467. doi:10.1016/0042-6822(73)90341-3

Gray, L., and A. Kreger. 1979. Microscopic characterization of rabbit lung damage produced by *Pseudomonas aeruginosa* proteases. *Infect. Immun.* 23:150–159.

Grigoryan, T., P. Wend, A. Klaus, and W. Birchmeier. 2008. Deciphering the function of canonical Wnt signals in development and disease: conditional loss- and gain-of-function mutations of beta-catenin in mice. *Genes Dev.* 22:2308–2341. doi:10.1101/gad.1686208

Holmes, C., and W.L. Stanford. 2007. Concise review: stem cell antigen-1: expression, function, and enigma. *Stem Cells*. 25:1339–1347. doi:10.1634/stemcells.2006-0644

Kalin, T.V., I.C. Wang, L. Meliton, Y. Zhang, S.E. Wert, X. Ren, J. Snyder, S.M. Bell, L.J. Graf Jr., J.A. Whitsett, and V.V. Kalinichenko. 2008. Forkhead Box m1 transcription factor is required for perinatal lung function. *Proc. Natl. Acad. Sci. USA*. 105:19330–19335. doi:10.1073/pnas.0806748105

Kim, C.F., E.L. Jackson, A.E. Woolfenden, S. Lawrence, I. Babar, S.M. Vogel, D. Crowley, R.T. Bronson, and T. Jacks. 2005b. Identification of bronchioalveolar stem cells in normal lung and lung cancer. *Cell*. 121:823–835. doi:10.1016/j.cell.2005.03.032

Kim, I.M., S. Ramakrishna, G.A. Gusarova, H.M. Yoder, R.H. Costa, and V.V. Kalinichenko. 2005a. The forkhead box m1 transcription factor is essential for embryonic development of pulmonary vasculature. *J. Biol. Chem.* 280:22278–22286. doi:10.1074/jbc.M500936200

Kobayashi, Y. 2008. The role of chemokines in neutrophil biology. *Front. Biosci.* 13:2400–2407. doi:10.2741/2853

Liu, Y., and B.L. Hogan. 2002. Differential gene expression in the distal tip endoderm of the embryonic mouse lung. *Gene Expr. Patterns.* 2:229–233. doi:10.1016/S1567-133X(02)00057-1

Liu, Y., H. Jiang, H.C. Crawford, and B.L. Hogan. 2003. Role for ETS domain transcription factors Pea3/Erm in mouse lung development. *Dev. Biol.* 261:10–24. doi:10.1016/S0012-1606(03)00359-2

Ma, T., N. Fukuda, Y. Song, M.A. Matthay, and A.S. Verkman. 2000. Lung fluid transport in aquaporin-5 knockout mice. *J. Clin. Invest.* 105:93–100. doi:10.1172/JCI8258

Mason, R.J. 2006. Biology of alveolar type II cells. *Respirology.* 11:S12–S15. doi:10.1111/j.1440-1843.2006.00800.x

Metzger, D.E., M.T. Stahlman, and J.M. Shannon. 2008. Misexpression of ELF5 disrupts lung branching and inhibits epithelial differentiation. *Dev. Biol.* 320:149–160. doi:10.1016/j.ydbio.2008.04.038

Mirza, M.K., Y. Sun, Y.D. Zhao, H.H. Potula, R.S. Frey, S.M. Vogel, A.B. Malik, and Y.Y. Zhao. 2010. FoxM1 regulates re-annealing of endothelial adherens junctions through transcriptional control of β-catenin expression. *J. Exp. Med.* 207:1675–1685. doi:10.1084/jem.20091857

Mucenski, M.L., J.M. Nation, A.R. Thitoff, V. Besnard, Y. Xu, S.E. Wert, N. Harada, M.M. Taketo, M.T. Stahlman, and J.A. Whitsett. 2005. Beta-catenin regulates differentiation of respiratory epithelial cells in vivo. *Am. J. Physiol. Lung Cell. Mol. Physiol.* 289:L971–L979. doi:10.1152/ajplung.00172.2005

Paine, R. III, and R.H. Simon. 1996. Expanding the frontiers of lung biology through the creative use of alveolar epithelial cells in culture. *Am. J. Physiol.* 270:L484–L486.

Perl, A.K., S.E. Wert, A. Nagy, C.G. Lobe, and J.A. Whitsett. 2002. Early restriction of peripheral and proximal cell lineages during formation of the lung. *Proc. Natl. Acad. Sci. USA.* 99:10482–10487. doi:10.1073/pnas.152238499

Raiser, D.M., and C.F. Kim. 2009. Commentary: Sca-1 and cells of the lung: a matter of different sorts. *Stem Cells.* 27:606–611. doi:10.1002/stem.10

Rawlins, E.L., and B.L. Hogan. 2006. Epithelial stem cells of the lung: privileged few or opportunities for many? *Development.* 133:2455–2465. doi:10.1242/dev.02407

Rawlins, E.L., T. Okubo, Y. Xue, D.M. Brass, R.L. Auten, H. Hasegawa, F. Wang, and B.L. Hogan. 2009a. The role of Scgb1a1+ Clara cells in the long-term maintenance and repair of lung airway, but not alveolar, epithelium. *Cell Stem Cell.* 4:525–534. doi:10.1016/j.stem.2009.04.002

Rawlins, E.L., C.P. Clark, Y. Xue, and B.L. Hogan. 2009b. The Id2+ distal tip lung epithelium contains individual multipotent embryonic progenitor cells. *Development.* 136:3741–3745. doi:10.1242/dev.037317

Reddy, R., S. Buckley, M. Doerken, L. Barsky, K. Weinberg, K.D. Anderson, D. Warburton, and B. Driscoll. 2004. Isolation of a putative progenitor subpopulation of alveolar epithelial type 2 cells. *Am. J. Physiol. Lung Cell. Mol. Physiol.* 286:L658–L667. doi:10.1152/ajplung.00159.2003

Rice, W.R., J.J. Conkright, C.L. Na, M. Ikegami, J.M. Shannon, and T.E. Weaver. 2002. Maintenance of the mouse type II cell phenotype in vitro. *Am. J. Physiol. Lung Cell. Mol. Physiol.* 283:L256–L264.

Sadikot, R.T., H. Zeng, M. Joo, M.B. Everhart, T.P. Sherrill, B. Li, D.S. Cheng, F.E. Yull, J.W. Christman, and T.S. Blackwell. 2006. Targeted immunomodulation of the NF-kappaB pathway in airway epithelium impacts host defense against *Pseudomonas aeruginosa*. *J. Immunol.* 176:4923–4930.

Sano, H., and Y. Kuroki. 2005. The lung collectins, SP-A and SP-D, modulate pulmonary innate immunity. *Mol. Immunol.* 42:279–287. doi:10.1016/j.molimm.2004.07.014

Stripp, B.R. 2008. Hierarchical organization of lung progenitor cells: is there an adult lung tissue stem cell? *Proc. Am. Thorac. Soc.* 5:695–698. doi:10.1513/pats.200801-011AW

Sugahara, K., J. Tokumine, K. Teruya, and T. Oshiro. 2006. Alveolar epithelial cells: differentiation and lung injury. *Respirology.* 11:S28–S31. doi:10.1111/j.1440-1843.2006.00804.x

Wang, X., K. Krupczak-Hollis, Y. Tan, M.B. Dennewitz, G.R. Adami, and R.H. Costa. 2002. Increased hepatic Forkhead Box M1B (FoxM1B) levels in old-aged mice stimulated liver regeneration through diminished p27Kip1 protein levels and increased Cdc25B expression. *J. Biol. Chem.* 277:44310–44316. doi:10.1074/jbc.M207510200

Ware, L.B., and M.A. Matthay. 2000. The acute respiratory distress syndrome. *N. Engl. J. Med.* 342:1334–1349. doi:10.1056/NEJM200005043421806

Wert, S.E., S.W. Glasser, T.R. Korfhagen, and J.A. Whitsett. 1993. Transcriptional elements from the human SP-C gene direct expression in the primordial respiratory epithelium of transgenic mice. *Dev. Biol.* 156:426–443. doi:10.1006/dbio.1993.1090

Wierstra, I., and J. Alves. 2006. FOXM1c transactivates the human c-myc promoter directly via the two TATA boxes P1 and P2. *FEBS J.* 273:4645–4667. doi:10.1111/j.1742-4658.2006.05468.x

Willis, B.C., J.M. Liebler, K. Luby-Phelps, A.G. Nicholson, E.D. Crandall, R.M. du Bois, and Z. Borok. 2005. Induction of epithelial-mesenchymal transition in alveolar epithelial cells by transforming growth factor-beta1: potential role in idiopathic pulmonary fibrosis. *Am. J. Pathol.* 166:1321–1332. doi:10.1016/S0002-9440(10)62351-6

Zhang, Y., A.M. Goss, E.D. Cohen, R. Kadzik, J.J. Lepore, K. Muthukumaraswamy, J. Yang, F.J. DeMayo, J.A. Whitsett, M.S. Parmacek, and E.E. Morrisey. 2008. A Gata6-Wnt pathway required for epithelial stem cell development and airway regeneration. *Nat. Genet.* 40:862–870. doi:10.1038/ng.157

Zhao, Y.Y., Y. Liu, R.V. Stan, L. Fan, Y. Gu, N. Dalton, P.H. Chu, K. Peterson, J.J. Ross Jr., and K.R. Chien. 2002. Defects in caveolin-1 cause dilated cardiomyopathy and pulmonary hypertension in knockout mice. *Proc. Natl. Acad. Sci. USA.* 99:11375–11380. doi:10.1073/pnas.172360799

Zhao, Y.Y., X.P. Gao, Y.D. Zhao, M.K. Mirza, R.S. Frey, V.V. Kalinichenko, I.C. Wang, R.H. Costa, and A.B. Malik. 2006. Endothelial cell-restricted disruption of FoxM1 impairs endothelial repair following LPS-induced vascular injury. *J. Clin. Invest.* 116:2333–2343. doi:10.1172/JCI27154